

Short communication

## Development of a stack having an optimized flow field structure with low cross transport effects

J. Scholta\*, F. Häussler, W. Zhang, L. Küppers, L. Jörissen, W. Lehnert

*Zentrum für Sonnenenergie- und Wasserstoff-Forschung, GB 3: Elektrochemische Energiespeicherung und -wandlung, Helmholtzstr. 8, D-89081 Ulm, Germany*

Received 4 February 2004; accepted 9 May 2005

Available online 1 September 2005

### Abstract

PEM fuel cells when operated on hydrogen from renewable sources are viewed as one of the most environmentally friendly energy conversion systems due to their high electrical efficiency. However, this advantage is depending on the overall system design, which is largely determined by the allowable operating conditions of the fuel cell stack itself. Besides the active materials, design and shape of the gas distribution zone have a significant influence on stack operation. In order to optimize overall system performance, a fuel cell stack with improved flow field design and performance was developed. An investigation on channel geometries led to a serpentine flow field with a moderate degree of parallelization and ribs with variable width to reduce cross transport effects. The resulting flow field subsequently has been modified slightly to allow a high volume production process. Summarizing, power as well as the degrees of H<sub>2</sub> and air utilization could be enhanced leading to a power density enhancement. Furthermore, weight reduction of end plates nearly by half using an improved end plate design led to an overall improved stack design.

© 2005 Elsevier B.V. All rights reserved.

*Keywords:* Fuel cell; PEMFC; Flow field design; Rib and channel geometry; Cross transport effects

### 1. Introduction

ZSW is developing PEM fuel cell stacks for use in portable power generation and stationary applications since 1995. Stacks with 50 cells having an active area of 100 cm<sup>2</sup> per cell resulting in a total power output up to 1.4 kW have been built and operated successfully. A power density of up to 0.3 W cm<sup>-2</sup> at an averaged single cell voltage of 0.6 V has been obtained, however, at comparatively low gas utilization. From a system point of view, it is evident, that hydrogen and air utilization is of great influence to the overall system efficiency. In this work, the influence of flow direction, flow field geometry and channel geometries on the stack performance have been studied, and experimental results on

the effects of relative flow direction and flow field geometry will be reported. Additional studies on the influence of channel geometries are in progress and will be reported elsewhere [1].

### 2. Experimental procedures

Starting from ZSWs standard configuration (internal manifold, cross flow), an experimental investigation on the influence of media flow directions and channel geometry has been carried out. A total of 10 different five-cell short stacks with varying width and depth of the flow channels and width of the ribs separating the channels were built and tested. Commercially available membrane electrode assemblies (MEA) and gas diffusion layers (GDL) were used. Stacks made from the previous standard design (cross flow) were tested as a reference. The experimental work was accompanied by CFD modeling using FLUENT<sup>TM</sup> software.

\* Corresponding author. Tel.: +49 731 9530 206; fax: +49 731 9530 666.

E-mail address: [joachim.scholta@zsw-bw.de](mailto:joachim.scholta@zsw-bw.de) (J. Scholta).

URL: <http://www.zsw-bw.de>.

### Nomenclature

dp	dew point
$X_{an}$	anode gas utilization, given as ratio between converted and supplied amount of hydrogen
$X_{ca}$	cathode gas utilization, given as ratio between converted and supplied amount of oxygen (in air)

### 2.1. Basic stack design

The flow fields to be investigated were machined in blank graphite composite plates. Anode and cathode side gas distribution fields were machined in separate plates. Each cell contained a cooling water distribution field, which was machined into the cathode plate. Separate metal ring gaskets having a screen printed silicon layer were used allowing to seal the anode and cathode part of the bipolar plate as well as an easy interchange of MEAs. The active area has been  $100 \text{ cm}^2$  in all cases. Both, serpentine (anode and cathode) and pattern type (anode) flow fields were investigated for gas distribution. GORE PRIMEA 5620 MEAs having a platinum loading of  $0.3 \text{ mg cm}^{-2}$  at the anode and  $0.4 \text{ mg cm}^{-2}$  at the cathode side were used as MEA. SGL 10 BB material was used as GDL.

Although in the initial phase reported here, the bipolar plates used were still machined, the final design can easily be adapted to a compression molding process.

### 2.2. Test bench

The cell performance was determined using a test bench developed at ZSW in cooperation with hydrogen-systems. The test bench layout is described in [2].

The test bench allows measurement and recording of all relevant experimental parameters (stack and single cell voltages, current, temperatures and pressures). Moreover, high frequency resistance (HFR) data at a frequency of 1 kHz can be recorded online in order to determine effects related to water management and cell construction. Gas humidification is achieved by passing the premixed reactant gases through a heated and isolated bubbler.

### 2.3. Test procedures

The stacks were tested using pure hydrogen as a fuel and air as an oxidant. Furthermore, tests using synthetic reformat have also been carried out. However, since no Pt/Ru catalysts were used, CO was not added to the simulated reformat. Normal operating conditions were as follows:  $T_{\text{Stack}} = 55\text{--}60 \text{ }^\circ\text{C}$ , ambient outlet pressure, dry anode gas, cathode inlet dew point  $45 \text{ }^\circ\text{C}$ . Hydrogen utilization 70%, air utilization 25%.

The tests were carried out under variation of the operating temperature, gas composition and gas utilization at anode and cathode side.

## 3. Results and discussion

For the development process reported here, the channel and rib geometries were fixed between 0.7 and 1.0 mm, respectively. These values have been selected based on a survey of the literature [3–5] as well as on model studies performed at ZSW. The results of these studies on the influence of rib and channel dimensions were experimentally tested and will be reported in [1].

### 3.1. Comparison of flow directions

Concerning the relative media flow direction, co-, cross- and counter flow designs were evaluated. The configuration scheme of flow directions is shown in Fig. 1. The scheme should illustrate the flow pathways and is not drawn to scale.

All performance data are given as mean single cell voltage dependent on current density or gas utilization. The performance dependency on flow directions for partially humidified gas streams was found to be increasing from co- to cross- and counter flow. Fig. 2 shows the dependence of cell performance on flow directions for co- and counter flow.

Cross flow conditions were examined as well. They showed an intermediate performance compared to co- and counter flow. If dry anode gas and humidified cathode gas have been used, counter flow turned out to be the best configuration as well for current versus voltage as well as for voltage utilization characteristics. The corresponding cathode utilization voltage characteristic shows a cell voltage of 0.580 V at an air utilization of 30% for co-flow, whereas for counter

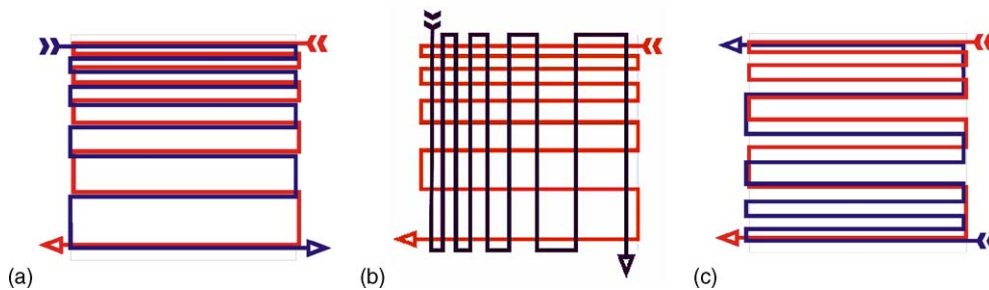


Fig. 1. Flow direction schemes for: (a) co-flow, (b) cross flow and (c) counter flow.

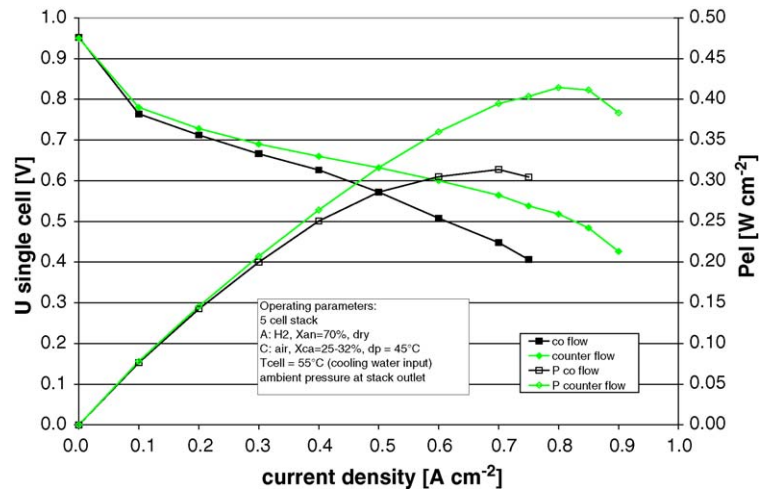


Fig. 2. Influence of flow directions on stack performance.

flow the same cell voltage was measured at an air utilization of 35%. It is assumed, that the advantageous behaviour of counter flow configurations is caused by a more even humidity distribution in the cell. Therefore, all further variations of channel geometry were investigated using a counter flow configuration.

Fig. 3 shows the dependence of current–voltage curves on flow field geometry.

When comparing performance data of flow fields having the same number of parallel channels, the flow fields having a larger depth are showing also a higher cell voltage, especially if high current densities are applied. It is assumed that this effect is caused by a reduction of cross transport in a serpentine flow field with respect to lower pressure differences. Increasing the number of parallel channels normally leads to a reduction in the cell voltage at moderate or low gas utilization because the effect of inlet pressure reduction

(at a fixed outlet pressure) outnumbers the effect a lowered cross transport at serpentine borders. However, highly parallel flow fields are typically showing a good performance even at high current densities. Furthermore, good utilization characteristics are achieved using a larger number of parallel channels. In the case of a single gas channel, the cell performance is significantly decreased as compared to medium and even high parallelization degree which is supposed to be caused by enhanced cross transport.

Summarizing these data it is assumed that the lack of performance in flow fields of low degree of parallelization can be attributed to a transport process including both cross flow and cross diffusion between the serpentine channels, particularly at their turning point which leads to media depleted zones. It can be concluded from the experimental data that the optimum number of parallel channels is dependent on flow field dimensions and geometries, pressure drop and flow rates.

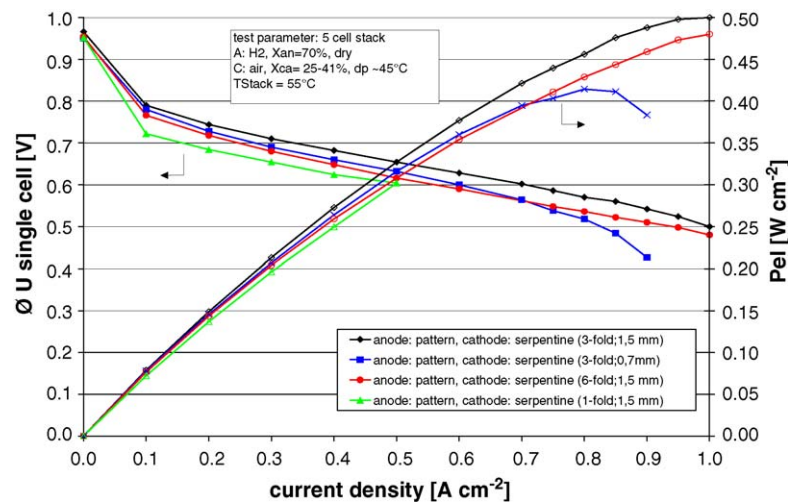


Fig. 3. Five-cell stack performance dependent on different flow field geometries.

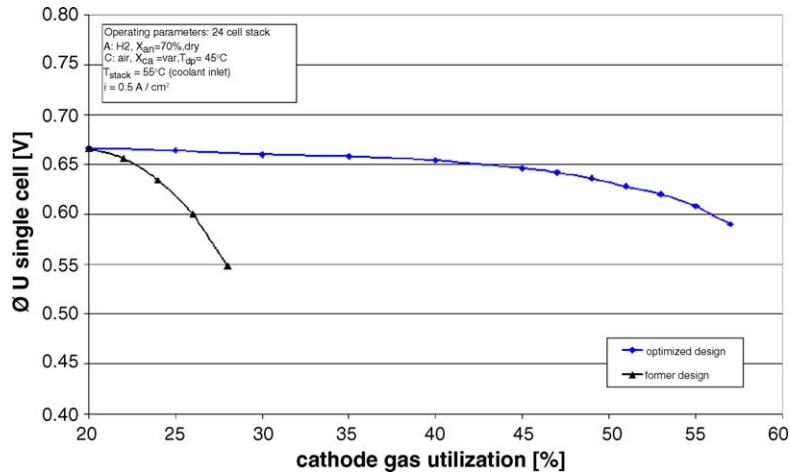


Fig. 4. Air utilization voltage curve for the optimized stack design compared to the former design.

These parameters should be selected to be high enough to get acceptable pressure differences and low cross transport losses on one hand and low enough in order to obtain sufficiently high gas flow velocities to remove condensate droplets from the cell.

Moreover, it can be concluded that a rib design, which reduces cross transport is desirable. A stack having three parallel gas distribution channels at a channel depth of 1.5 mm has been selected for further variations of the rib design.

From a system efficiency point of view, the tolerable anode gas utilization must be above 90% for hydrogen and more than 70% for steam reformat. Dependent on the pressure difference of the cell, a cathode air utilization of more than 35% should be achieved. Fig. 4 shows the corresponding air utilization voltage curve compared to the former standard stack concept. To overcome at least a part of the problems caused by cross transport effects, the ribs which separate gas flow in opposite direction are designed in a way shown in Fig. 5.

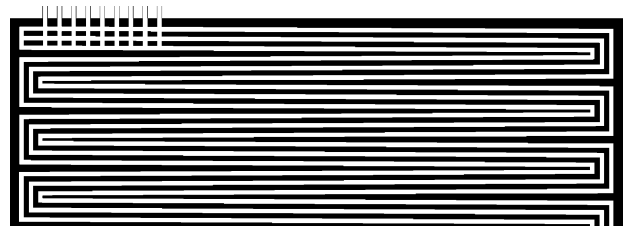


Fig. 5. Flow field design showing ribs with variable rib width across a border channel.

The rib width at the turning points of the media flow was varied between 1.2 and 2.4 mm. The voltage utilization curves are given in Fig. 6.

A maximum rib width of 1.8 mm was identified as the best compromise for a good performance at high as well as at lower degrees of gas utilization. The different and partially lower voltages at lower air utilization degrees for cells having wedge ribs at the serpentine borders may be due to a

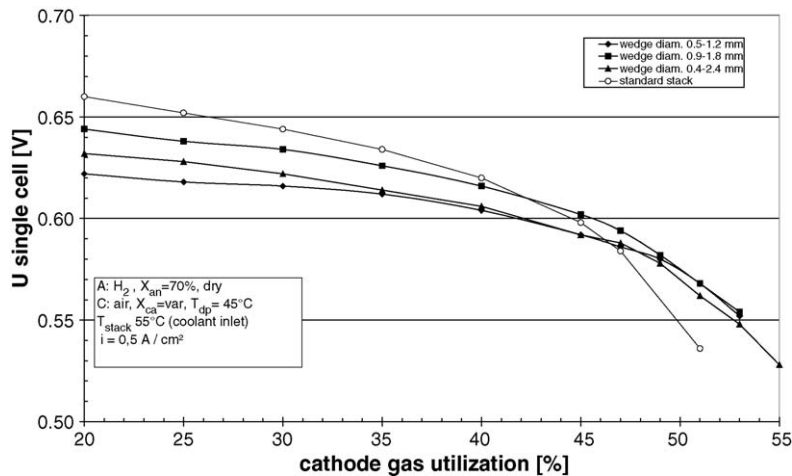


Fig. 6. Cathode gas utilization characteristic for different wedge rib stacks (five cells).



Fig. 7. Twenty-four-cell stack with non-machined bipolar plates under test.

higher rib overlap between anode and cathode in the standard configuration. More details on possible designs are given in [6]. Since the reactant distribution is significantly depending on the gas diffusion layer thickness and porosity [7], the presented design should be adapted if other GDL types are used.

### 3.2. Adaptation to a design compatible with volume manufacturing

Starting from the initial design variations (performance data shown in Fig. 3), the flow fields were adapted to channel and rib geometries compatible with compression moulding without suffering loss in performance. A 24-cell stack is shown in Fig. 7. A corresponding current voltage curve is shown in Fig. 8.

Using the optimized flow field design, a power output of more than  $36 \text{ W cell}^{-1}$  (hydrogen) at an averaged cell voltage

of  $600 \text{ mV}$  can be reached corresponding to a power density of  $360 \text{ mW cm}^{-2}$  in a 24-cell stack with atmospheric outlet pressure conditions. Using reformat ( $x(\text{H}_2) = 0.35$  or  $0.5$ ), a cell power of 30 or more  $\text{W cell}^{-1}$  was measured. The sustained stack specific power (hydrogen) amounts to  $\sim 0.15 \text{ kW kg}^{-1}$ , the power density is approximately  $\sim 0.3 \text{ kW l}^{-1}$ . Summarizing, the specific data of the optimized stack with an active area of  $100 \text{ cm}^2$  is comparable to those of the stack with  $560 \text{ cm}^2$  active area as reported in [2].

### 3.3. Pressure drop

All stacks show an almost linear flow pressure characteristic. A pressure drop of  $57 \text{ mbar NI}(\text{H}_2)^{-1} \text{ min}^{-1} \text{ cell}^{-1}$  was measured at the anode side, the corresponding value at the cathode side amounts to  $77 \text{ mbar NI}(\text{air})^{-1} \text{ min}^{-1} \text{ cell}^{-1}$ .

### 3.4. CFD calculations

No scaling effects concerning uniformity of cell voltages have been observed when the performance of the 24-cell stack is compared to 5-cell short stacks. Nonetheless, CFD calculations have been used to check if a uniformity of flow rates (and cell voltage in consequence) could be expected for stacks having an even larger number of cells. The gas flow in the manifold channels as well as in the inlet and outlet sections of the individual cells was fully modelled. The flow resistance of the individual cell gas distribution zones, which previously has been modelled by experimentally confirmed CFD calculations were approximated by a flow resistor term. Fig. 9 shows the resulting flow rates and pressure distributions, leading to the conclusion that using the design presented above, it is possible to build stacks up to 150 cell with low and up to 200 cells with acceptable deviations from flow (and therefore voltage) uniformity.

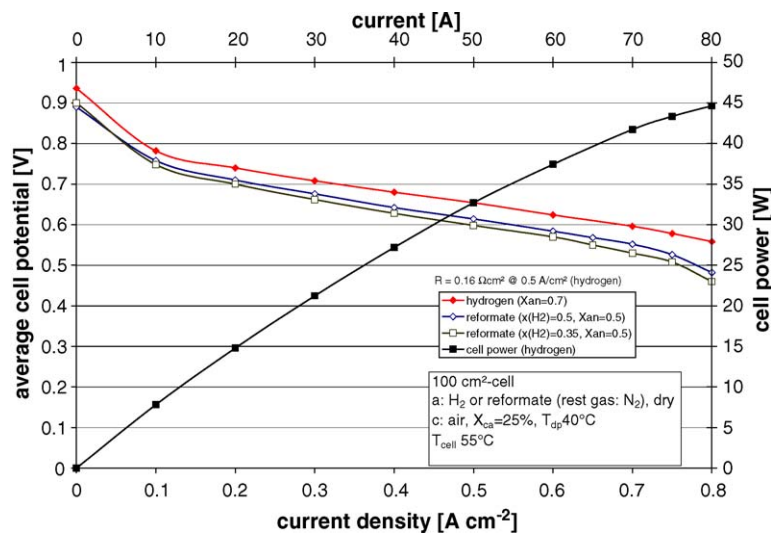


Fig. 8. Current voltage curve for the 24-cell stack (reformat: 5-cell stack).

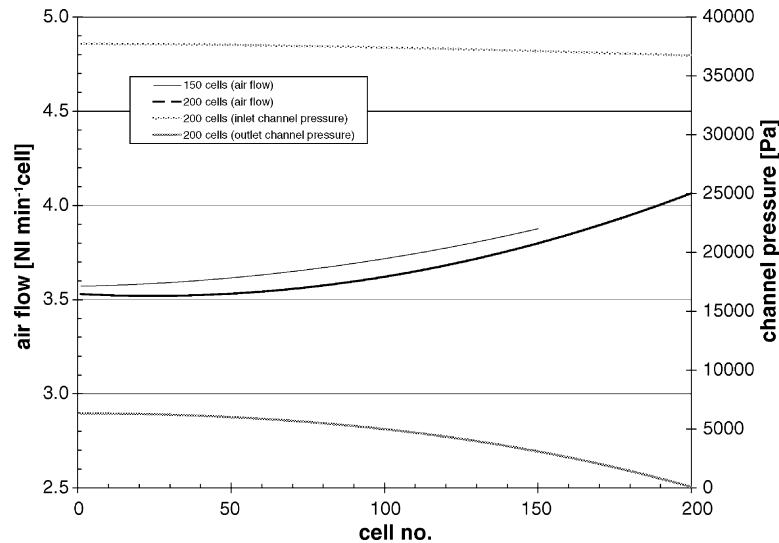


Fig. 9. Cell flow rates and pressure distribution for a 150 and 200-cell stack.

### 3.5. End plate design

The end plates were designed allowing manufacturing by either machining or casting. The design was carried out in such a way that:

- the end plate is not connected electrically to the fuel cell potential;
- the current collector has no contact to media.

All media connectors were led to a single side. The current collectors in the final stack were made from a gold plated non-ferrous metal. The design of the end plate has been optimized with respect to weight reduction by reduction of plate thickness and use of high strength aluminum. A weight reduction of 50% could be achieved.

## 4. Summary and conclusion

A PEM fuel cell stack design operating close to ambient pressure has been developed. A flow field design optimization was performed which lead to increased power and gas utilization characteristics. No scale effects with respect to cell number were observed. It is expected that stacks consisting of 150 cells or more can be built. The design concept was successfully adapted to a fabrication process compatible with volume manufacturing, such that first steps in cost reduction also have been demonstrated. Further tests with respect to performance and lifetime of the stack are in progress and will be published elsewhere.

## Acknowledgements

The project was carried out in cooperation with a manufacturer of carbon materials. The project was financially supported by the MWMEV (state of NRW, Germany) with confirmation date of May 17, 2001.

## References

- J. Scholta, G. Escher, W. Zhang, L. Küppers, L. Jörissen, W. Lehnert, Investigation on the influence of channel geometries on PEMFC performance, *J. Power Sources* 155 (2006) 66–71.
- J. Scholta, N. Berg, P. Wilde, L. Jörissen, J. Garche, Development and performance of a 10 kW PEMFC stack, *J. Power Sources* 127 (2004) 206–212.
- P.L. Hental, J.B. Lakeman, G.O. Mepsted, P.L. Adcock, New materials for polymer electrolyte membrane fuel cell current collectors, *J. Power Sources* 80 (1999) 235–241.
- T.-H. Yang, L. Won, H.-M. Jung, Y.-G. Yoon, J.-S. Park, K. Chang, Optimization of channel dimensions in gas distributor for polymer electrolyte membrane fuel cell (PEFC), in: 2nd European PEFC Forum Proceedings, vol. 1, European Fuel Cell Forum, Oberrohrdorf, Luzern, CH, June 30–July 4, 2003, pp. 239–244, ISBN 3-905592-13-4.
- K.T. Jeng, S.F. Lee, G.F. Tsai, C.H. Wang, Oxygen mass transfer in PEM fuel cell gas diffusion layers, *J. Power Sources* 138 (2004) 41–50.
- L. Jörissen, J. Scholta, F. Häussler, W. Zhang, W. Lehnert, Gas flow field for a fuel cell and a fuel cell containing such a gas flow field (ger.), DE Patent 10 2004 026 134 A1.
- H.-K. Lee, J.-H. Park, Do.-Y. Kim, T.-H. Lee, A study on the characteristics of the diffusion layer thickness and porosity of the PEMFC, *J. Power Sources* 131 (2004) 200–206.